Kinetics of Acid-Catalyzed Breakdown of Spiro Meisenheimer Complexes[1]

Claude F. Bernasconi* and Keith A. Howard

Contribution from the Thimann Laboratories of the University of California, Santa Cruz, California 95064. *Received August 30, 1982. Revised Manuscript Received March 11, 1983*

Abstract: The breakdown of spiro Meisenheimer complexes derived from 1-(2-hydroxyethoxy)-2,6-dinitro-4-X-benzene is catalyzed by carboxylic acids and by H_3O^+ but catalysis by substituted pyridinium ions is weak or undetectable. This contrasts with a previous report on the breakdown of 1,1-dimethoxy-2,6-dinitro-4-X-cyclohexadienates which is strongly catalyzed by substituted pyridinium ions but only weakly catalyzed by carboxylic acids. This different response to catalyst charge indicates a different balance in the degree of proton transfer and C–O bond breaking in the transition state for the two types of complexes. Just as for the noncatalyzed reaction studied previously the acid-catalyzed breakdown of the spiro complexes is intrinsically faster than that of the 1,1-dimethoxy complexes which is attributed to a stereoelectronic effect. However, the difference in intrinsic reactivity is smaller for the catalyzed compared to the noncatalyzed pathway, and this difference decreases with increasing acidity of the catalyst. This indicates a transition state in which there is less p–π overlap, i.e., a transition state which is more complex-like in the catalyzed reactions. This conclusion is consistent with the observation of less negative ρ_n values (variation of 4-X substituent) in the catalyzed reactions. Brønsted α values for the spiro complexes are 0.49 ± 0.01 for X = H, 0.51 ± 0.02 for X = Cl, 0.54 ± 0.02 for X = CF_3, 0.56 ± 0.01 for X = NO_2, and 0.58 ± 0.01 for X = SO_2CF_3. This increasing trend in α with increasing electron-withdrawing strength of the X substituent is in qualitative agreement with that observed for the 1,1-dimethoxy complexes and is easily rationalized as the result of both a parallel and a perpendicular effect on a More O'Ferrall–Jencks energy surface. There are indications that *quantitatively* the substituent effect on α is smaller for the spiro ($p_{xy} \approx 0.010 \pm 0.002$) than for the 1,1-dimethoxy complexes ($p_{xy} \approx 0.016 \pm 0.001$) although a possible slight dependence of p_{xy} on the X substituent renders this conclusion somewhat uncertain. Possible reasons as to why p_{xy} might be different in the two systems are discussed.

It has been known for some time that the ring opening of spiro Meisenheimer complexes is significantly faster than the loss of methoxide ion from comparable 1,1-dimethoxy complexes, despite the higher thermodynamic stability of the spiro complexes.[1a,2-4] This indicates that the intrinsic reactivity ("intrinsic barrier"[5]) is much higher (lower) for the spiro complex reactions.

The fact that one of the reactions is intramolecular makes a *quantitative* assessment of the difference in intrinsic reactivity somewhat difficult. In a recent paper[1a] we addressed this problem and described a procedure for making the two reactions thermodynamically comparable by correcting rate and equlibrium constants for the intramolecularity of spiro complex formation and by making an allowance for the slight difference in the pK_a^{ROH} values of the respective alcohols. The results for the complexes derived from 2,6-dinitro-4-X-anisoles (eq 1) and from 1-(2-hydroxyethoxy)-2,6-dinitro-4-X-benzenes (eq 2) in aqueous solution are summarized in Table I. $K_1^{ad,corr}$(**4-X**), $k_1^{ad,corr}$(**4-X**), and $k_{-1}^{ad,corr}$(**4-X**) refer to the constants that have been *adjusted* for the different pK_a values and *corrected* for intramolecularity, while $\Delta\Delta G^{\ddagger} = \Delta G^{\ddagger}(k_1)_{2\text{-}X} - \Delta G^{\ddagger}(k_1^{ad,corr})_{4\text{-}X}$.

The two major conclusions to be drawn from Table I are that the difference in intrinsic reactivity between the two families is quite large ($\Delta\Delta G^{\ddagger}$ = 3.80–5.34 kcal/mol) and that this difference increases as the X substituent becomes more electron withdrawing. We have shown that the most likely cause for the difference in reactivity is of stereoelectronic origin.[1a] Thus, in the spiro complexes the orientation of the lone-pair orbitals on the oxygens is such as to lead to p–π overlap in the transition state. On the other hand, in the 1,1-dimethoxy complexes the orientation of the lone-pair orbitals does not lead to such overlap unless the complex first undergoes an unfavorable conformational change.

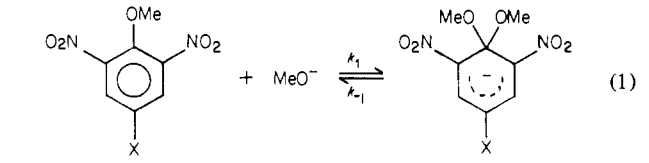

1-X **2-X** (1)

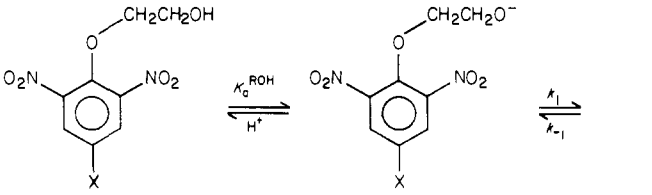

3-X

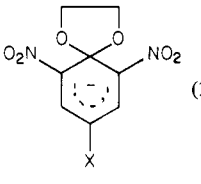

(2)

4-X

The fact that $\Delta\Delta G^{\ddagger}$ increases with the electron-withdrawing strength of the X substituent supports this interpretation because p–π overlap leads to a transfer of charge density from the nonreacting oxygen into the benzene ring, a process that is facilitated by stronger electron-withdrawing groups.

In this paper we wish to examine how the change from a 1,1-dimethoxy to a spiro complex affects the general acid–base catalyzed reactions 3 and 4. Extensive data on reaction 3 have

$$\textbf{1-X} + \text{MeOH} + \text{B}^z \underset{k_{-1}^{BH}}{\overset{k_1^B}{\rightleftharpoons}} \textbf{2-X} + \text{BH}^{z+1} \quad (3)$$

$$\textbf{3-X} + \text{B}^z \underset{k_{-1}^{BH}}{\overset{k_1^B}{\rightleftharpoons}} \textbf{4-X} + \text{BH}^{z+1} \quad (4)$$

already been reported[6] but only one member of the **4-X** family

(1) (a) Part 22 of the series Intermediates in Nucleophilic Aromatic Substitution. Part 21: Bernasconi, C. F.; Howard, K. A. *J. Am. Chem. Soc.* **1982**, *104*, 7248. (b) Preliminary account of this work: Bernasconi, C. F., Howard, K. A. *Bull. Soc. Chim. Belg.* **1982**, *91*, 405.

(2) For a recent review, see: Terrier, F. *Chem. Rev.* **1982**, *82*, 77.

(3) Crampton, M. R.; Willison, M. J. *J. Chem. Soc., Perkin Trans. 2* **1974**, 1681.

(4) Bernasconi, C. F.; Gandler, J. R. *J. Org. Chem.* **1977**, *42*, 3387.

(5) (a) Marcus, R. A. *J. Phys. Chem.* **1968**, *72*, 891. (b) Cohen, A. O.; Marcus, R. A. *Ibid.* **1968**, *72*, 4249. (c) Hine, J. *J. Am. Chem. Soc.* **1971**, *93*, 3701. (d) Albery, W. J. *Annu. Rev. Phys. Chem.* **1980**, *31*, 227.

(6) Bernasconi, C. F.; Gandler J. R. *J. Am. Chem. Soc.* **1978**, *100*, 8117.

0002-7863/83/1505-4690$01.50/0

Table I. Comparison between Spiro and 1,1-Dimethoxy Complexes after Adjustment for the Difference in pK_a^{ROH} and Correction for Intramolecularity. Noncatalyzed Reactions[a]

	H	Cl	CF_3	NO_2	SO_2CF_3
$\frac{k_1^{ad,corr}(4\text{-X})}{k_1(2\text{-X})} = \frac{k_{-1}^{ad,corr}(4\text{-X})}{k_{-1}(2\text{-X})}$	6.20×10^2	9.04×10^2	3.42×10^3	7.26×10^3	8.40×10^3
$\Delta\Delta G^{\ddagger}$, kcal/mol	3.80	4.02	4.81	5.25	5.34
$K_1^{ad,corr}(4\text{-X}) = K_1(2\text{-X})$	1.27×10^{-6}	1.00×10^{-4}	3.89	3.53×10^4	5.16×10^5
ΔG°, kcal/mol	8.02	5.44	−0.80	−6.18	−7.77

[a] From ref 1a.

Table II. Summary of Rate Constants for the Breakdown of Spiro Complexes (4-X) at 25 °C, μ = 0.2 M

rate constant (pK_a^{BH})[a]	H (4.25)[b]	Cl (64.4)[b]	CF_3 (3.25×10^4)[b]	NO_2 (5.69×10^7)[b]	SO_2CF_3 (4.09×10^8)[b]
k_{-1},[c] s^{-1}	137	50.5	4.30	0.10	8.90×10^{-2}
k_{-1}^{AcOH}, M^{-1} s^{-1} (4.67)	538	260	29.0	0.87	0.86
k_{-1}^{HCOOH}, M^{-1} s^{-1} (3.60)	1880		82.1	2.21	
$k_{-1}^{MeOAcOH}$, M^{-1} s^{-1} (3.45)	1910	775	122	3.79	3.01
k_{-1}^{ClAcOH}, M^{-1} s^{-1} (2.71)	4930	2380	350	19.3	10.5
k_{-1}^{CNAcOH}, M^{-1} s^{-1} (2.32)	7410	3560	662	16.9	20.0
k_{-1}^{PyH}, M^{-1} s^{-1} (5.40)	314				
k_{-1}^{NicH},[d] M^{-1} s^{-1} (3.42)	1100				
$k_{-1}^{3\text{-Cl-PyH}}$, M^{-1} s^{-1} (2.92)	1890				
k_{-1}^{H}, M^{-1} s^{-1} (−1.74)	2.25×10^5	2.10×10^5	3.93×10^4	1400	1440
k_{-1}^{BH},[e] M^{-1} s^{-1} (5.00)	371	188	19.4	0.56	0.52

[a] Determined potentiometrically at μ = 0.2 M (KCl). [b] Number in parentheses is $K_1 = k_1/k_{-1}$ (eq 2), from ref 1a. [c] From ref 1a. [d] Nic = nicotinamide. [e] BH is a hypothetical carboxylic acid of pK_a = 5.00.

Table III. Brønsted α Values for Acid-Catalyzed Breakdown of Meisenheimer Complexes

		Spiro Complexes (Carboxylic Acids)			
substituent	H[a]	Cl	CF_3	NO_2	SO_2CF_3
α	0.49 ± 0.01	0.51 ± 0.02	0.54 ± 0.02	0.56 ± 0.01	0.58 ± 0.01
K_1	4.25	64.4	3.25×10^4	5.69×10^7	4.08×10^8
		1,1-Dimethoxy Complexes (Pyridinium Ions)[b]			
substituent	CF_3	CN	SO_2CH_3	NO_2	SO_2CF_3
α	0.55 ± 0.01	0.58 ± 0.01	0.59 ± 0.01	0.61 ± 0.02	0.63 ± 0.02
K_1	3.89	6.44×10^2	*c*	3.53×10^4	5.16×10^5

[a] α = 0.38 ± 0.01 for catalysis by pyridinium ions. [b] Reference 6. [c] Not determined.

has been studied[7] (X = NO_2). We now report a kinetic investigation of the acid-catalyzed breakdown of **4-X** with X = H, Cl, CF_3, NO_2 (reinvestigation), and SO_2CF_3.

Results

Rates of acid-catalyzed breakdown were measured for five spiro complexes **4-X** (X = H, Cl, CF_3, NO_2, SO_2CF_3). The procedure involved in situ generation of the complex by placing **3-X** into a basic solution (typically 0.01 M KOH) and then mixing it with an acidic buffer or an HCl solution in the stopped-flow apparatus. The rates were determined spectrophotometrically by monitoring the decay of the complex between 400 and 575 nm. All experiments were conducted under pseudo-first-order conditions at 25 °C and at an ionic strength of 0.2 M (KCl). The pH of the final solution was always low enough as to make the reaction virtually irreversible.

Since the breakdown of the 1,1-dimethoxy complexes has been studied with substituted pyridinium ion catalysts,[6] the use of the same catalysts would have been desirable in the present case. We found, however, that except for the reaction of **4-H**, catalysis by pyridinium ions is either undetectable or too weak to allow the determination of a meaningful catalytic rate constant. On the other hand, catalysis by carboxylic acids which are inefficient catalysts for the 1,1-dimethoxy complexes[6] is easily measurable for spiro complex breakdown. Most of our data were therefore obtained with carboxylic acids.

In all cases the observed pseudo-first-order rate constants obeyed eq 5; they are summarized elsewhere[8] (201 rate constants). The

$$k_{obsd} = k_{-1} + k_{-1}^{H}a_{H^+} + k_{-1}^{BH}[BH] \quad (5)$$

catalytic rate constants, k_{-1}^{BH}, were obtained from the slopes of plots of k_{obsd} vs. [BH]. The range of [BH] was typically 0.01 to 0.1 or 0.2 M and the plots consisting of five to six points gave excellent straight lines. Rate enhancements over $k_{-1} + k_{-1}^{H}a_{H^+}$ were typically as much as twofold at [BH] = 0.2 M, leaving little doubt that the observed accelerations represent authentic general acid catalysis rather than salt effects. This conclusion is supported by experiments at high ionic strength (0.36 M), which showed only miniscule changes in k_{-1}^{BH}, and by the results of Crampton and Willison[7] for **4-NO_2** when a different (NaCl) compensating electrolyte is used.[9]

The rate constants for the noncatalyzed (k_{-1}) and the hydronium ion catalyzed reactions (k_{-1}^{H}) were obtained from the intercepts of the buffer plots and from additional runs in HCl solutions; k_{-1} was found to agree very well with the values measured previously in alkaline solutions.[1a]

Table II provides a summary of all catalytic rate constants, the k_{-1} values, and equilibrium constants, K_1.

Discussion

Mechanism. Figure 1 shows representative Brønsted plots for catalysis by carboxylic acids. In most cases we found a slight deviation for formic acid from the line defined by acetic, methoxyacetic, chloroacetic, and cyanoacetic acid, consistent with

(7) Crampton, M. R.; Willison, M. J. *J. Chem. Soc., Perkin Trans. 2* **1974**, 1686.

(8) Howard, K. A. Ph.D. Thesis, University of California, Santa Cruz, 1982.

(9) Catalysis of substituted pyridinium ions which could only be measured for **4-H** is somewhat more sensitive to changes in ionic strength and to the nature of the compensating electrolyte. For example, k_{-1}^{BH} for pyridinium ion catalysis is 314, 261, and 206 M^{-1} s^{-1} at μ = 0.2, 0.36, and 0.5 M, respectively, a trend which follows classical theory for a reaction between two oppositely charged ions. Furthermore, a change from KCl to NaCl lowers k_{-1}^{BH} for nicotinamide catalysis by 15%.

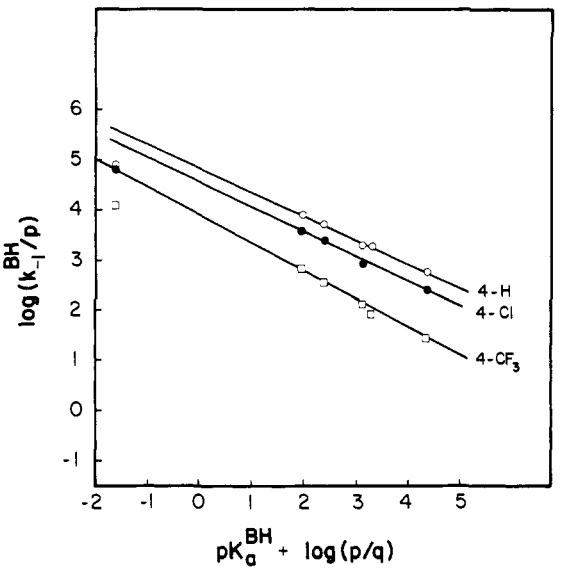

Figure 1. Representative Brønsted plots for acid-catalyzed breakdown of some spiro complexes. Data from Table II.

findings by Crampton and Willison[7] and also with those of Capon and Nimmo for acetal hydrolysis.[10] For **4-NO$_2$** we also found a slight positive deviation with chloroacetic acid. In calculating α values the deviating points were omitted.

Brønsted α values are summarized in Table III along with the α values for the 1,1-dimethoxy complexes;[6] they span a range from 0.38 (see footnote *a* in Table III) to 0.58 which is typical for concerted reactions.[11] Other evidence that reactions such as eq 3 and 4 represent a concerted process has been summarized recently.[6]

With respect to the H^+-catalyzed pathway, solvent isotope effects indicate that it also follows a concerted mechanism[6,7] rather than an A1 mechanism.[12] An interesting question is whether or not this concerted mechanism is enforced[11,13] by an impossibly short lifetime of the protonated Meisenheimer complex (**4H-X**). The question can be answered by estimating the order of magnitude of k_H for the hypothetical A1 mechanism shown in eq 6.

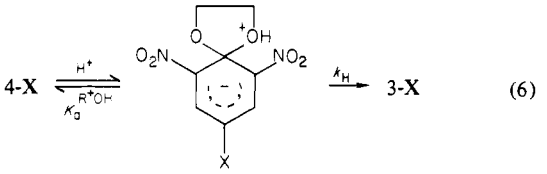

If the k_{-1}^H process were to represent an A1 mechanism, k_{-1}^H would be given by $k_H/K_a^{R^+OH}$ and thus $k_H = K_a^{R^+OH}k_{-1}^H$. However, since the actual mechanism is concerted, the A1 mechanism must be a less favorable pathway which implies $k_H < (\ll) K_a^{R^+OH}k_{-1}^H$, i.e., $K_a^{R^+OH}k_{-1}^H$ represents only an upper limit for k_H. $pK_a^{R^+OH}$ can be estimated to be between ca. −3.2 (X = H) and −4.1 (X = SO_2CF_3) as detailed below in the section entitled Corrections for Intramolecularity and Construction of Energy Diagrams. Hence, on the basis of the k_{-1}^H values summarized in Table II, $K_a^{R^+OH}k_{-1}^H$ is estimated to be between $\approx 3.6 \times 10^8$ s^{-1} for X = H and $\approx 1.8 \times 10^7$ s^{-1} for X = SO_2CF_3. This shows that k_H is several orders of magnitude below 10^{13} s^{-1} which is usually considered to be the upper limit for a viable species.[11,13] Hence **4H-X** exists as a relatively stable species[14] and concerted H^+ catalysis is not enforced.

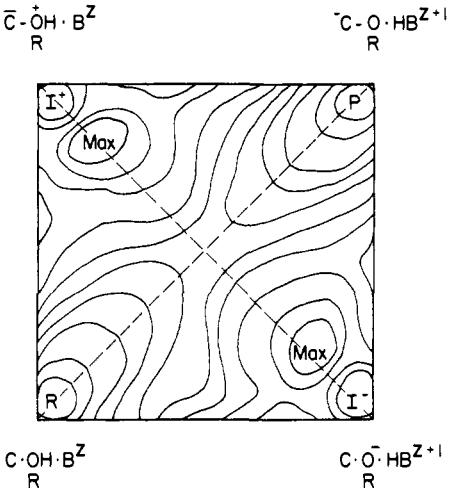

Figure 2. Schematic representation of a MOFJ diagram for the reaction of an aromatic substrate (C) with an alcohol to form a Meisenheimer comlex ($^-$C–OR). There are three potential wells along the I^-–I^+ diagonal, see text.

Similar conclusions apply to the 1,1-dimethoxy complexes studied previously (X = CF_3, CN, SO_2CH_3, NO_2, SO_2CF_3); this probably even holds for **2-H** which is too unstable to be studied by our methods but for which $K_a^{R^+OH}k_{-1}^H$ can be estimated (see below) by extrapolation to be $\approx 3.5 \times 10^{11}$ s^{-1}.

Our findings are thus similar to those recently reported by Palmer and Jencks[15] in the dehydration of a carbinolamine. They have a bearing on how these reactions are to be represented on a More O'Ferrall–Jencks (MOFJ) energy diagram.[16,17] A schematic representation of such a diagram is shown in Figure 2. As pointed out by Palmer and Jencks, the existence of a protonated intermediate such as **4H-X** (I^+ corner in Figure 2) shows that in this type of reaction it is possible to have three potential wells along the diagonal cross section from the lower right (I^-) to the upper left (I^+) corner as indicated in the figure. This is an important conclusion in view of theoretical arguments which seem to disfavor the existence of three potential wells in similar energy diagrams.[18,19]

With respect to the mechanism of the k_{-1} process, we believe, just as with the 1,1-dimethoxy complexes,[6] that it represents simple alkoxide ion departure rather than concerted catalysis by water. The fact that the points for $k_{-1}/[H_2O]$ deviate positively from the Brønsted plots by factors of 10^3 or more supports the notion of a different mechanism for this reaction. Additional arguments have been presented elsewhere.[6]

Electrostatic Effects. The fact that the neutral carboxylic acids are more effective catalysts than the cationic pyridinium ions indicates that electrostatic effects in the transition state are important.[19] Two types of electrostatic effects need to be considered. One is the interaction of the charge on the catalyst ($+\delta$ for cationic catalysts, $-\delta$ for neutral catalysts) with the overall charge on the complex ($-\delta$). The other is the interaction between the charge on the catalyst and the developing charge on the departing oxygen. The charge on oxygen may be either positive, negative, or nil, depending on the relative progress of proton transfer vs. C–O bond breaking in the transition state. If the charge on the departing oxygen is relatively large (positive or negative), this second type of interaction is likely to dominate, but if this charge is small or zero, the first type of interaction is expected to be more important.

On the basis of the above considerations, the experimental observations for the spiro complexes are consistent with substantial

(10) Capon, B.; Nimmo, K. *J. Chem. Soc., Perkin Trans. 2* **1975**, 1113.
(11) Jencks, W. P. *Acc. Chem. Res.* **1976**, *9*, 425.
(12) Cordes, E. H.; Bull, H. G. *Chem. Rev.* **1974**, *74*, 581.
(13) Jencks, W. P. *Acc. Chem. Res.* **1980**, *13*, 161.
(14) An additional condition for **4H-X** to exist is that there is a barrier for the loss of the proton to the solvent. Palmer and Jencks[15] have discussed this problem and argued convincingly that such a barrier does exist for species such as protonated alcohols, ethers, etc.
(15) Palmer, J. L.; Jencks, W. P. *J. Am. Chem. Soc.* **1980**, *102*, 6466.
(16) More O'Ferrall, R. A. *J. Chem. Soc. B* **1970**, 274.
(17) (a) Jencks, W. P. *Chem. Rev.* **1972**, *72*, 705. (b) Jencks, D. A.; Jencks, W. P. *J. Am. Chem. Soc.* **1977**, *99*, 7948.
(18) See, e.g.: (a) Albery, W. J. *Prog. React. Kinet.* **1967**, *4*, 353. (b) Gandour, R. D.; Maggiora, G. M.; Schowen, R. L. *J. Am. Chem. Soc.* **1974**, *96*, 6967. (c) Gandour, R. D., personal communication.
(19) See, e.g.: Kresge, A. J.; Chiang, Y. *J. Am. Chem. Soc.* **1973**, *95*, 803.

Table IV. Normalized ρ Values for the Breakdown of Meisenheimer Complexes

			Spiro Complexes			
catalyst	H_2O	BH[b]	AcOH	$MeOCH_2COOH$	$NCCH_2COOH$	H_3O^+
ρ_n[a]	−0.40	−0.36	−0.36	−0.35	−0.34	−0.30
			1,1-Dimethoxy Complexes			
catalyst	H_2O	BH^+ [c]	$PicH^+$ [d]	PyH^+	$NicH^+$	H_3O^+
ρ_n[a]	−0.53	−0.46	−0.49	−0.47	−0.44	−0.37

[a] Estimated error ±0.01. [b] BH is a hypothetical carboxylic acid with $pK_a = 5.00$. [c] BH^+ is a hypothetical pyridinium ion catalyst with $pK_a = 5.00$. [d] Pic = picoline.

Table V. β_{1g} Values ($\beta_{1g} = \alpha + \rho_n$) for Catalyst of $pK_a^{BH} = 5.00$

			Spiro Complexes		
substituent	H	Cl	CF_3	NO_2	SO_2CF_3
β_{1g}	0.13	0.15	0.19	0.20	0.22
			1,1-Dimethoxy Complexes		
substituent	CF_3	CN	SO_2CH_3	NO_2	SO_2CF_3
β_{1g}	0.09	0.12	0.13	0.15	0.17

positive charge development on the departing oxygen as shown in **5** for carboxylic acids (effective catalysts) and in **6** for pyridinium ions (ineffective catalysts). For the 1,1-dimethoxy complexes the opposite situation prevails in that it is the cationic catalysts that are more efficient. This suggests that there is either very little charge on the departing oxygen so that interaction of the overall negative charge of the complex with that of the catalyst dominates or that there is some negative charge on the departing oxygen as shown in **7** and **8**.

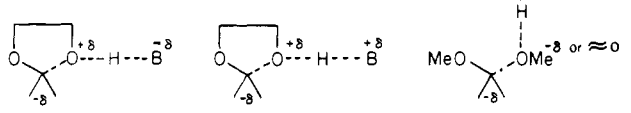

5 6 7

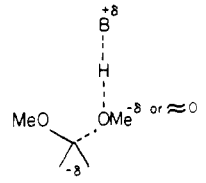

8

The above conclusions are supported by our findings for H^+ catalysis. In the reactions which are measurably catalyzed by pyridinium ions (all **2-X** and **4-H**) the point for k_{-1}^H lies on the Brønsted line defined by the other positively charged catalysts, while in the reactions catalyzed by carboxylic acids the point for k_{-1}^H deviates negatively from the Brønsted line.

Structure–Reactivity Coefficients. The Brønsted α values are summarized in Table III, along with those for the 1,1-dimethoxy complexes. We have also obtained normalized ρ values, defined as $\rho_n = \partial \log k_{-1}^{BH}/\partial \log K_1$.[20] They are summarized in Table IV for each catalyst, again for both families of complexes.

The values obtained for α and ρ_n appear to support our conclusions about the charge distribution in the various transition states (**5–8**). The common interpretation of α is that it measures how much positive charge has been transferred from the catalyst to the complex while ρ_n is a measure of the fraction of negative charge which has been removed from the benzene ring. In the idealized situation where these structure–reactivity parameters are an *exact* measure of the mentioned charges one expects β_{1g} (eq 7)[6] to correspond to the charge on the departing oxygen, in

$$\beta_{1g} = \alpha + \rho_n \qquad (7)$$

which case the transition state is said to be "balanced".[17b] This ideal is probably rarely achieved; in the case of 1,1-dimethoxy complexes, β_{1g} obtained directly by measuring breakdown rates

(20) $\partial \log k_{-1}^{BH}/\partial \log K_1$ is equivalent to $(\partial \log k_{-1}^{BH}/\partial\sigma^-)/\rho_{eq}$.

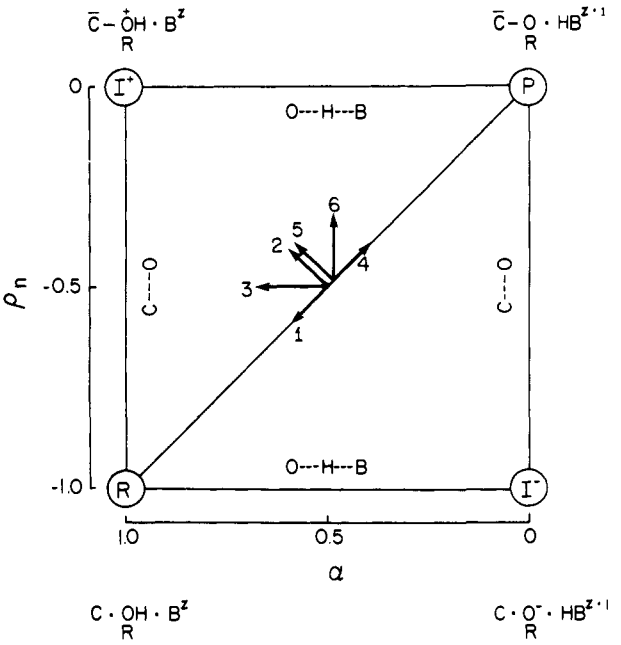

Figure 3. MOFJ diagram from which contour lines have been omitted. Arrows 1 + 2 = 3 show the effect of making the X substituent more electron withdrawing; arrows 4 + 5 = 6 show the effect of making the catalyst more acidic.

of **9** as a function of R ($\beta_{1g} = \partial \log k_{-1}^{BH}/\partial pK_a^{ROH}$) provides an independent, though approximate,[21] measure of the charge developing on the departing oxygen.[6] The agreement between this

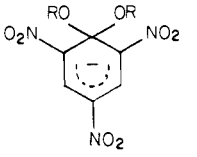

9

directly measured β_{1g} and $\alpha + \rho_n$ is not very good (e.g., for BH = pyridinium ion $\alpha + \rho_n = 0.61-0.47 = +0.14$ while $\partial \log k_{-1}^{BH}/\partial pK_a^{ROH} = -0.05$[6]), indicating an imbalanced transition state. Hence $\alpha + \rho_n$ should not be regarded as a measure of absolute charge but it is probably a valid measure of *relative* charge in comparing the different complexes with each other.

Table V summarizes β_{1g} values calculated via eq 7 for both families of complexes referring to a hypothetical standard catalyst of $pK_a^{BH} = 5.00$. We note that, as a family, the spiro complexes have somewhat larger β_{1g} values, indicating a more positive charge on the departing oxygen. This is in agreement with our previous conclusion based on catalyst charge type. In the same vein it is also noteworthy that **4-H**, which is the only spiro complex whose breakdown is measurably catalyzed by pyridinium ions, is the one with the lowest β_{1g} value.

The dependence of α on the X substituent, and the dependence of ρ_n on the catalyst, is easily understood in the context of a More O'Ferrall–Jencks diagram. For convenience we have redrawn such

(21) Since R on both oxygens was changed simultaneously β_{1g} obtained from $\partial \log k_{-1}^{BH}/\partial\ pK_a^{ROH}$ can only be an approximate measure of this change.[6]

Table VI. Rate Constants and $\Delta G^{\ddagger}$ Values (Adjusted and Corrected for Spiro Complexes) for Breakdown of Complexes

row no.		H[a]	Cl[a]	CF_3	NO_2	SO_2CF_3	X[b]
			1,1-Dimethoxy Complexes[a]				
1	k_{-1}, s^{-1}	5.76×10^2	57.4	1.34×10^{-1}	4.96×10^{-4}	2.56×10^{-4}	1.05×10^{-6}
2	$\Delta G^{\ddagger}(k_{-1})$, kcal/mol	13.6	15.0	18.6	21.9	22.3	25.6
3	$k_{-1}^{BH}(pK_a^{BH} = 5.0)$, M^{-1} s^{-1}	1.93×10^4	2.53×10^3	27.4	1.38×10^{-1}	1.10×10^{-1}	3.98×10^{-4}
4	$\Delta G^{\ddagger}(k_{-1}^{BH})$, kcal/mol	11.6	12.8	15.5	18.6	18.7	22.0
5	k_{-1}^{H}, M^{-1} s^{-1}	2.24×10^7	5.25×10^6	2.40×10^5	3.40×10^3	3.30×10^3	56.0
6	$pK_a^{R^+OH}$	−4.20	−4.43	−4.74	−4.98	−5.13	−5.50
7	$K_a^{R^+OH}k_{-1}^{H}$, s^{-1}	3.53×10^{11}	1.41×10^{11}	1.32×10^{10}	3.25×10^8	4.45×10^8	1.77×10^7
8	$\Delta G^{\ddagger}(k_H)$, kcal/mol	>1.70	>2.24	>3.64	>5.83	>5.64	>7.55
			Spiro Complexes				
9	k_{-1}, s^{-1}	1.37×10^2	50.5	4.3	0.10	8.90×10^{-2}	2.50×10^{-3}
10	k_{-1}^{ad}, s^{-1}	21.7	8.00	6.81×10^{-1}	1.58×10^{-2}	1.41×10^{-2}	3.94×10^{-4}
11	EM_{eq}^{c}, M	3.37×10^7	6.44×10^6	8.35×10^4	1.61×10^4	7.93×10^3	5.60×10^2
12	$k_{-1}^{ad,corr}$, s^{-1}	3.56×10^5	5.20×10^4	4.58×10^2	3.58	2.15	1.37×10^{-2}
13	$\Delta G^{\ddagger}(k_{-1}^{ad,corr})$, kcal/mol	9.84	11.0	13.8	16.6	16.9	19.9
14	$k_{-1}^{BH}(pK_a^{BH} = 5.0)$, M^{-1} s^{-1}	3.71×10^2	1.88×10^2	19.4	0.56	0.52	2.51×10^{-2}
15	$k_{-1}^{BH,ad}$, M^{-1} s^{-1}	1.66×10^2	84.5	8.72	0.25	0.23	1.13×10^{-2}
16	$k_{-1}^{BH,ad,corr}$, M^{-1} s^{-1}	4.04×10^5	9.80×10^4	1.43×10^3	19.7	13.3	1.94×10^{-1}
17	$\Delta G^{\ddagger}(k_{-1}^{BH})$, kcal/mol	9.70	10.6	13.1	15.6	15.9	18.4
18	k_{-1}^{H}, M^{-1} s^{-1}	2.25×10^5	2.10×10^5	3.93×10^4	1.40×10^3	1.44×10^3	1.00×10^2
19	$k_{-1}^{H,ad}$, M^{-1} s^{-1}	5.92×10^5	5.52×10^5	1.03×10^5	3.68×10^3	3.79×10^3	2.63×10^2
20	$k_{-1}^{H,ad,corr}$, M^{-1} s^{-1}	3.61×10^8	1.82×10^8	6.82×10^6	1.32×10^5	1.05×10^5	2.73×10^3
21	$pK_a^{R^+OH}$	−3.20	−3.43	−3.74	−3.98	−4.13	−4.50
22	$K_a^{R^+OH}k_{-1}^{H,ad,corr}$, s^{-1}	4.99×10^{11}	4.90×10^{11}	3.75×10^{10}	1.26×10^9	1.42×10^9	8.62×10^7
23	$\Delta G^{\ddagger}(k_H)$, kcal/mol	>1.50	>1.50	>3.03	>5.03	>4.96	>6.62

[a] For the dimethoxy complexes rate constants etc. were obtained by extrapolation; see text. [b] X is a hypothetical substituent with $\sigma^- \approx 1.8$ which gives $K_1 = 10^{10}$ for the dimethoxy complex. [c] From ref 1a.

a diagram in Figure 3 by omitting the contour lines from Figure 2. Inspection of Figure 3 shows that a change to a more electron-withdrawing X substituent, which stabilizes the complex, has the effect of lowering the energy of the entire upper horizontal edge. This induces an uphill shift of the saddle point along the reaction coordinate toward the R corner (arrow 1) and a perpendicular downhill shift toward the top left intermediate (I^+) corner (arrow 2).[22] The resulting vector (arrow 3) implies that proton transfer has made more progress in the transition state, as is borne out by an increase in the observed Brønsted α values (Table III).

Again with reference to Figure 3 one can visualize that the effect of increasing the acidity of the catalyst is to raise the right edge of the diagram. This induces the parallel and perpendicular shifts indicated by arrows 4 and 5, respectively, with the overall result shown as arrow 6.[22] The resulting effect is to increase ρ_n (to less negative values), as observed (Table IV).

It should be noted that the changes in α with the X substituent, and the changes in ρ_n with the catalyst, are interrelated by the cross correlation coefficient p_{xy};[17b] in its normalized form it is given by [23]

$$p_{xy} = \partial\alpha/\partial \log K_1 = -\partial\rho_n/\partial pK_a^{BH} \quad (8)$$

(K_1 is the equilibrium constant for reactions 1 and 2; K_1 values are in Table III).

Figure 4 shows plots of α vs. log K_1 for both families of complexes. For the present we shall assume that these plots represent straight lines even though there might be some curvature in one or both plots, a point which will be dealt with at the end of this paper. With the assumption that the lines are straight the slopes

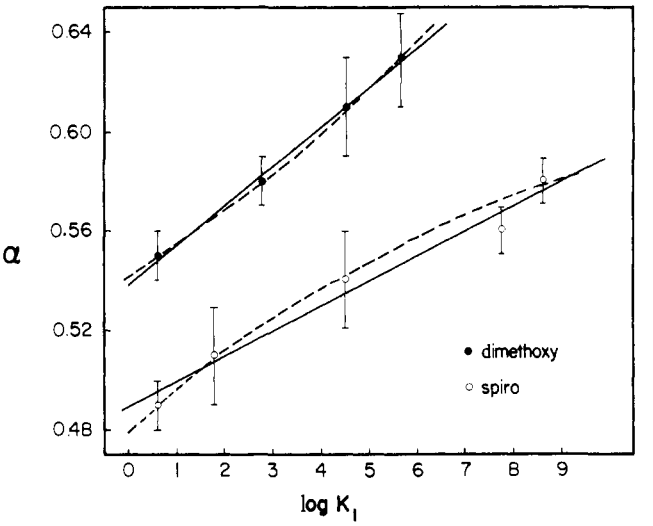

Figure 4. Dependence of Brønsted α values on the stability constant (K_1) of Meisenheimer complexes. Data from Table III.

(p_{xy}) appear to be significantly different from each other: p_{xy} = 0.010 ± 0.002 for the spiro and 0.016 ± 0.001[24] for the 1,1-dimethoxy complexes. The p_{xy} values calculated as $-\partial\rho_n/\partial pK_a^{BH}$ are the same, within experimental error, as they should be, but the experimental errors are larger since they are based on only three points which span a relatively small reactivity range.

The question as to why p_{xy} might be smaller for the spiro complexes than for the 1,1-dimethoxy complexes is an interesting one. At the end of this paper we shall offer some speculative thoughts regarding this problem.

Corrections for Intramolecularity and Construction of Energy Diagrams. In order to compare intrinsic reactivities between the two families of complexes one needs to apply corrections for the intramolecularity of the spiro complex formation and for the

(22) As a matter of convenience we have arbitrarily placed the transition state of the reference reaction into the center of the diagram, represented the reaction coordinate as a perfect diagonal, and assumed that the parallel and perpendicular shifts are of the same magnitude which implies equal curvatures along and perpendicular to the reaction coordinate. These are idealizations which are unlikely to reflect the actual situation but unless they are grossly out of line the qualitative conclusions to be drawn are unaffected.

(23) $\partial\alpha/\partial \log K_1$ is equivalent to $(\partial\alpha/\partial\sigma^-)/\rho_{eq}$ where ρ_{eq} refers to the substituent dependence of K_1.[17b] Bypassing σ^- and ρ_{eq} is the preferred procedure here because of some ambiguities in choosing a proper set of σ^- values.[1a]

(24) p_{xy} for the 1,1-dimethoxy complexes differs slightly from the value of 0.014 published previously[6] because it is now based on experimental[1a] rather than estimated K_1 values.

approximately one unit lower pK_a^{ROH} of **3-X** compared to that of methanol.[1a] The correction procedures to be used are quite similar to the ones applied to the noncatalyzed reaction; since they have been discussed in great detail previously,[1a] only a brief description is given here.

(1) For the noncatalyzed pathway the experimental K_1 values for the spiro complexes (listed in Table III) are adjusted to the pK_a^{ROH} of methanol by multiplying them with a factor of 10, i.e., K_1^{ad}(**4-X**) = $10K_1$(**4-X**). This factor of 10 is based on the reasonable assumption that relative carbon basicities of oxyanions are proportional to their relative proton basicities.[25] This calls for a corresponding adjustment in k_1 and k_{-1}. We set $k_1^{ad} = k_1 \times 10^{0.2}$ and $k_{-1}^{ad} = k_{-1} \times 10^{-0.8}$; 0.2 (−0.8) corresponds to $\beta_{1g}(1 - \beta_{1g})$ obtained by measuring k_{-1} for the breakdown of **9** as a function of R.[6] The k_{-1} and k_{-1}^{ad} values are summarized in Table VI (rows 9 and 10 for spiro complexes, row 1 for the dimethoxy complexes).

(2) The ratio of K_1^{ad}(**4-X**)/K_1(**2-X**) is the equilibrium effective molarity,[26] EM_{eq}, of the spiro complex derived from an oxyanion of the same basicity as MeO^-; K_1(**2-X**) values are listed in Table III and EM_{eq} values in Table VI, row 11. It is now assumed that a hypothetical "*inter*molecular" spiro complex derived from such an oxyanion would have an adjusted and corrected equilibrium constant which is the same as that for the 1,1-dimethoxy complex, i.e., we need to multiply K_1^{ad}(**4-X**) by $(EM_{eq})^{-1}$ so that $K_1^{ad,corr}$(**4-X**) = $(EM_{eq})^{-1}K_1^{ad}$(**4-X**) = K_1(**2-X**). This correction for intramolecularity necessitates corresponding corrections in k_1^{ad} and k_{-1}^{ad}. We set $k_1^{ad,corr} = k_1^{ad}(EM_{eq})^{-\rho_n(k_1)}$ and $k_{-1}^{ad,corr} = k_{-1}^{ad}(EM_{eq})^{-\rho_n(k_{-1})}$ with $\rho_n(k_1) = 0.44$ and $\rho_n(k_{-1}) = -0.56$ referring to the reaction of **2-X**.[27] $k_{-1}^{ad,corr}$ values are in Table VI (row 12).

(3) In comparing the general acid catalyzed reactions (k_{-1}^{BH}) of the two complexes one needs to choose catalysts of the same pK_a^{BH} in order to assure that the thermodynamics of reactions 3 and 4 (after adjustment to the pK_a of methanol and correction for intramolecularity) are the same. We choose a hypothetical catalyst of $pK_a^{BH} = 5.0$ for which the "experimental" k_{-1}^{BH} values are easily found by interpolation from the respective Brønsted plots. Adjustment of k_{-1}^{BH}(**4-X**) to the pK_a of methanol leads to $k_{-1}^{BH,ad} = k_{-1}^{BH} \times 10^{-0.35}$ with −0.35 being β_{1g} for the breakdown of **9** catalyzed by an acid of $pK_a^{BH} = 5.0$.[6] Correction for intramolecularity leads to $k_{-1}^{BH,ad,corr} = k_{-1}^{BH,ad}(EM)_{eq}^{-\rho_n(k_{-1}^{BH})}$ with $\rho_n(k_{-1}^{BH}) = -0.45$ referring to the reaction of **2-X**.[27] Values for k_{-1}^{BH}, $k_{-1}^{BH,ad}$, and $k_{-1}^{BH,ad,corr}$ are in Table VI (rows 14–16).

(4) Adjustments and corrections for k_{-1}^{H}(**4-X**) for the H^+-catalyzed pathway are made in a similar way as for k_{-1}^{BH}(**4-X**): $k_{-1}^{H,ad} = k_{-1}^{H} \times 10^{0.42}$ with 0.42 being β_{1g} for the H^+-catalyzed breakdown of **9**,[6] and $k_{-1}^{H,ad,corr} = k_{-1}^{H,ad}(EM)_{eq}^{-\rho_n(k_{-1}^{H})}$ with $\rho_n(k_{-1}^{H}) = -0.37$ referring to the reaction of **2-X**.[27] Values for k_{-1}^{H}, $k_{-1}^{H,ad}$, and $k_{-1}^{H,ad,corr}$ are in Table VI (rows 18–20).

It needs to be understood that there is a certain arbitrariness in the choice of β_{1g} and ρ_n used to adjust and correct the rate constants, and the quantitative aspects of our results depend to some extent on it. However, as we have shown previously[1a] the *qualitative* conclusions are *not* sensitive to these choices.

From the data summarized in Table VI we can now calculate the free-energy changes associated with the various rate and equilibrium processes and assign relative energies to the corners, the edge barriers, and the central barriers in diagrams of the sort shown in Figure 2. For simplicity we shall ignore the fact that the species shown in the corners of the diagram are encounter complexes, i.e., the numbers to be derived are based on free species. Inasmuch as association may not be equally strong (differences in H-bond strength and electrostatic interactions) in the four corners this could introduce some error in their relative energies. However, these effects are expected to be too small to affect our conclusions. In the same vein we shall assume that the transition states along the vertical edges are not stabilized by hydrogen bonding or electrostatic effects with the catalyst.

We thus proceed as follows: (1) The R corner is the reference state (zero energy).

(2) The energy of the I^- corner is given by $2.3RT(pK_a^{ROH} - pK_a^{BH})$ with $pK_a^{ROH} = 15.5$, $pK_a^{BH} = 5.0$.

(3) The energy of the P corner is obtained by subtracting $2.3RT$ log K_1 from the energy of the I^- corner.

(4) The energy of the I^+ corner is calculated by adding $2.3RT(pK_a^{BH} - pK_a^{R^+OH})$ to the energy of the P corner with $pK_a^{R^+OH}$ referring to the protonated Meisenheimer complex. $pK_a^{R^+OH}$ is estimated as follows. The $pK_a^{R^+OH}$ of CH_3OCH_2-$^+OCH_3(H)$ is −4.57.[12] The 2,6-dinitro-4-X-cyclohexadienyl moiety is expected to be acidifying for strongly electron withdrawing X substituents, despite the negative charge in the ring. When X = NO_2 this effect amounts to at least 2 pK_a units for Meisenheimer complexes derived from amine nucleophiles.[28] In the present case the acidifying effect is assumed to be considerably less than that because it is likely to be compensated, in part, by a much stronger intramolecular hydrogen bond to one of the ortho nitro groups.[28,29] The estimated $pK_a^{R^+OH}$ values for the dimethoxy complexes are summarized in Table VI (row 6); for their dependence on the X substituent a Hammett $\rho = -1.0$ has been assumed.

For the *actual* spiro complexes $pK_a^{R^+OH}$ is expected to be about the same as for the 1,1-dimethoxy complexes since the inductive effect of the nonprotonated oxygen must be about the same in both complexes. This means that for the hypothetical "intermolecular" spiro complex for which pK_a^{ROH} has been increased by one unit over that of the actual complex, $pK_a^{R^+OH}$ must also be increased by one unit (Table VI, row 20). In calculating the energy of the I^+ corner we shall however assume equal $pK_a^{R^+OH}$ values for both families of complexes in order to make the corner energies the same. This is again a thermodynamic adjustment which will require a corresponding adjustment in the rate constants of the breakdown of the I^+ corner as discussed below.

(5) In estimating the horizontal edge barriers we assume a standard state of pH = 5.0 and [BH] = [B] = 1 M. Assuming diffusion-controlled proton transfer with rate constants in the thermodynamically favored direction of 10^{10} M^{-1} s^{-1},[30] one estimates the barrier at ≈3.8 kcal/mol above the energy of the I^- corner for the lower edge and at ≈3.8 kcal/mol above the energy of the I^+ corner for the upper edge.

(6) The energy of the transition states along the right vertical edge is found by adding $\Delta G^{\ddagger}(k_{-1})$ (1,1-dimethoxy complexes) and $\Delta G^{\ddagger}(k_{-1}^{ad,corr})$ (spiro complexes), respectively, to the P corner. For the saddle points one adds $\Delta G^{\ddagger}(k_{-1}^{BH})$ and $\Delta G^{\ddagger}(k_{-1}^{BH,ad,corr})$, respectively, to the energy of P corner.

(7) For the left vertical edge one can only estimate lower limits for the transition-state energies, based on $k_H < (\ll) K_a^{R^+OH}k_{-1}^{H}$, with k_H and $K_a^{R^+OH}$ referring to eq 6 or a similar equation for the 1,1-dimethoxy complexes. For these latter complexes the lower limits are then obtained by adding $\Delta G^{\ddagger}(K_a^{R^+OH}k_{-1}^{H})$ to the energy of the I^+ corner. For the spiro complexes, as mentioned under (4), an adjustment of $\Delta G^{\ddagger}$ is, at least in principle, called for to compensate for the adjusted I^+ corner. However, the transition-state energy is likely to be changing by about the same amount as the corner energy since the leaving group pK is not affected by the adjustment. Hence no adjustment to $\Delta G^{\ddagger}$ will be made, i.e., the transition-state energy is calculated by adding $\Delta G^{\ddagger}(K_a^{R^+OH}k_{-1}^{H,ad,corr})$ to the energy of the I^+ corner. Once again, whether the chosen procedure is strictly correct of not has no bearing on the conclusions drawn below.

Figure 5 shows a summary of the various free energies calculated as described above for the five spiro complexes studied and for the five corresponding 1,1-dimethoxy complexes (Figure 5A–E). The corners and edges are defined in the same way as in Figure 2; the numbers in parentheses refer to the spiro complexes. For **2-H** and **2-Cl** which could not be studied experimentally the

(25) Hine, J.; Weimar, R. D., Jr. *J. Am. Chem. Soc.* **1965**, *87*, 3387.
(26) Kirby, A. J. *Adv. Phys. Org. Chem.* **1980**, *17*, 183.
(27) Justification as to why ρ_n of the reaction of the 1,1-dimethoxy complexes rather than that of the spiro complexes is used is given in ref 1a.
(28) (a) Bernasconi, C. F.; Gehriger, C. L. *J. Am. Chem. Soc.* **1974**, *96*, 1092. (b) Bernasconi, C. F.; Muller, M. C.; Schmid, P. *J. Org. Chem.* **1979**, *44*, 3189.
(29) Bernasconi, C. F.; Terrier, F. *J. Am. Chem. Soc.* **1975**, *97*, 7458.
(30) Eigen, M. *Angew. Chem., Int. Ed. Engl.* **1964**, *3*, 1.

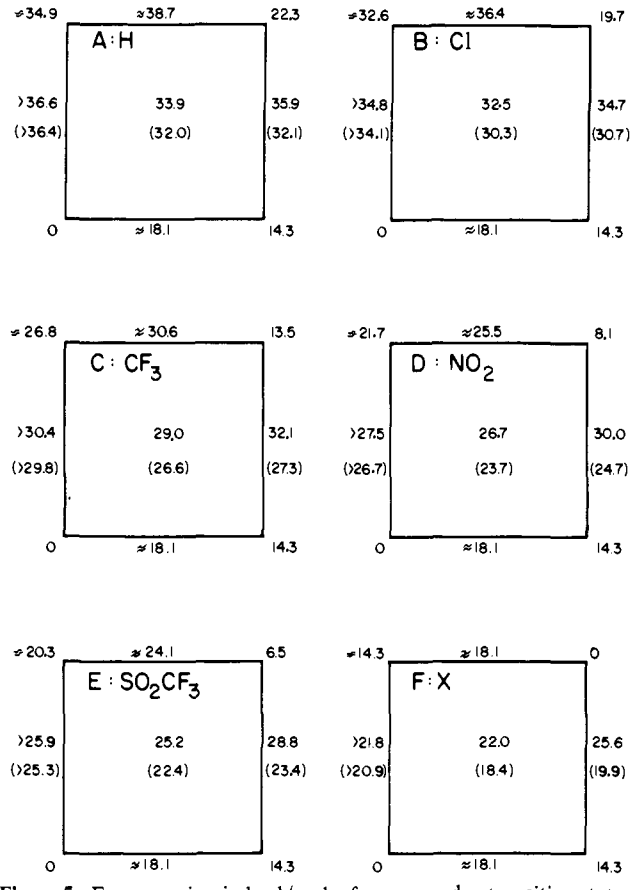

Figure 5. Free energies, in kcal/mol, of corners, edge transition states, and central transition states for 1,1-dimethoxy and for hypothetical "intermolecular" spiro Meisenheimer complexes. Values in parentheses refer to the spiro complexes. A–E, acutal X substituents; F, hypothetical X substituent for which $K_1 = 10^{10}$ ($\sigma^- \approx 1.8$).

reported values were obtained by suitable extrapolation from structure–reactivity plots. The figure also shows the relevant energies for a set of hypothetical complexes with a hypothetical X substituent whose σ^- value is about 1.8 (Figure 5F), again obtained by suitable extrapolations. This latter case is of particular interest because the energy diagrams are symmetrical in the sense that the R and P corners are of equal energy (zero) and the energies of the I^- and I^+ corners are equal to each other (14.3 kcal/mol).

Effect of Catalyst on Intrinsic Reactivity Difference between Spiro and 1,1-Dimethoxy Complexes. Inspection of Figure 5 allows the following conclusions to be drawn.

(1) Just as for the noncatalyzed pathway, the intrinsic barrier for the concerted acid-catalyzed pathway is lower in the spiro family. However, there is a quantitative reduction in the advantage of the spiro over the 1,1-dimethoxy complexes. For example, in the case shown in Figure 5F, $\Delta\Delta G^{\ddagger} = 22.0 - 18.4 = 3.6$ kcal/mol for the central barrier ($pK_a^{BH} = 5.0$) while $\Delta\Delta G^{\ddagger} = 25.6 - 19.9 = 5.7$ kcal/mol for the noncatalyzed reaction (right-edge barrier). Or for the other extreme shown in Figure 5A, $\Delta\Delta G^{\ddagger} = 1.9$ kcal/mol for the central barrier and $\Delta\Delta G^{\ddagger} = 3.8$ kcal/mol for the right-edge barrier. $\Delta\Delta G^{\ddagger}$ for the other cases are summarized in Table VII.

(2) The advantage of the spiro over the 1,1-dimethoxy complexes decreases further as the catalyst becomes more acidic. For the strongest catalyst, H_3O^+, the relevant $\Delta\Delta G^{\ddagger}$ are included in Table VII. They are seen to span a range from 1.6 to 2.3 kcal/mol.

(3) For the specific acid catalyzed pathway (left edge) the reactivity difference between the two families nearly disappears. Here $\Delta\Delta G^{\ddagger}$ spans a range from ≈0.9 to ≈0.2 kcal/mol (Table VII). These numbers are of course somewhat uncertain because they are based on the assumption that the lower limits estimated for these edge barriers are a fairly accurate reflection of the *relative* actual barriers.

Table VII. $\Delta\Delta G^{\ddagger}$ (kcal/mol) of Vertical-Edge Barriers and of the Central Barrier[a]

	H	Cl	CF_3	NO_2	SO_2CF_3	X[b]
right edge	3.8	4.0	4.8	5.3	5.4	5.7
central (BH)[c]	1.9	2.2	2.4	3.0	2.8	3.6
central (H_3O^+)[d]	1.6	2.1	2.0	2.2	2.0	2.3
left edge	≈0.2	≈0.7	≈0.6	≈0.8	≈0.7	≈0.9

[a] Taken from Figure 5. [b] Hypothetical substituent with $\sigma^- \approx 1.8$. [c] $pK_a^{BH} = 5.00$. [d] Data taken from Table VI.

The narrowing gap between the two families in the direction discussed above goes hand in hand with a trend toward less negative ρ_n values (Table IV). This trend in ρ_n indicates less transfer of negative charge from the benzene ring to the departing group, and thus also less C–O bond breaking, i.e., a transition state which is less product-like (**1-X**, **3-X**). This is consistent with our proposal that transition-state stabilization by p–π overlap between a lone-pair orbital of the nonreacting oxygen and the benzene ring is mainly responsible for the higher reactivity of the spiro complexes. According to this notion one expects that transition-state stabilization would be most effective when this p–π overlap can be maximized by having the C–O bond of the nonreacting oxygen relatively coplanar with the benzene ring (product-like transition state). Our results indeed show the expected parallelism between larger $\Delta\Delta G^{\ddagger}$ values and more product-like transition states (more negative ρ_n values).

The very small $\Delta\Delta G^{\ddagger}$ values estimated for the left edge suggest that the transition state strongly resembles the complex (I^+ corner).

Difference in p_{xy} Coefficients. As mentioned in an earlier section, p_{xy} for the spiro complexes (0.010 ± 0.002) seems lower than for the 1,1-dimethoxy complexes (0.016 ± 0.001), although this conclusion depends somewhat on the assumption that the plots of α vs. log K_1 (Figure 4) are linear. No firm conclusion can be reached at this point as to why such a difference in p_{xy} might exist. Nevertheless, we offer some speculative thoughts which may serve to stimulate further research.

As illustrated in Figure 3 the changes in transition-state structure can be understood as the vector sum of a parallel and a perpendicular shift on the energy surface. These shifts are commonly visualized as resulting from linear perturbations of the potential energy surface induced by the substituent change.[17b,31] The degree of shift for a given perturbation depends on the curvature along and perpendicular to the reaction coordinate. When the curvature is weak the shifts are large; when the curvature is strong the shifts are small. Hence one may attribute the smaller p_{xy} coefficient in the spiro series to a stronger curvature either along or/and perpendicular to the reaction coordinate.

There are a number of reasons why the curvatures might be different for the two families of complexes. One which seems particularly attractive is related to the difference in the barriers. How the difference in the barrier could affect curvature is most easily seen for the symmetrical case of Figure 5F. If one approximates the reaction coordinate by an inverted parabola,[31] the cross section through the energy surface along the reaction coordinate would be as shown in Figure 6A. The figure implies a somewhat stronger curvature for the 1,1-dimethoxy complex with a correspondingly shorter arrow 1 in Figure 3.

If everything else were equal this would lead to a smaller p_{xy} value for the 1,1-dimethoxy complexes. Since experimentally p_{xy} is *larger* one needs to assume that the stronger parallel curvature is overcompensated by an appreciably weaker perpendicular curvature (longer arrow 2). In view of the fact that perpendicular cross sections through the energy surface are triple-well potentials for which the height and location of the two maxima (Figure 2) are not known, we can only speculate as to how these cross sections would look. Figure 6B shows one of several possible situations which is consistent with the requirement of a weaker curvature for the 1,1-dimethoxy complexes. The result is summarized schematically in the following vector diagram (absolute lengths

(31) Thornton, E. R. *J. Am. Chem. Soc.* **1967**, *89*, 2915.

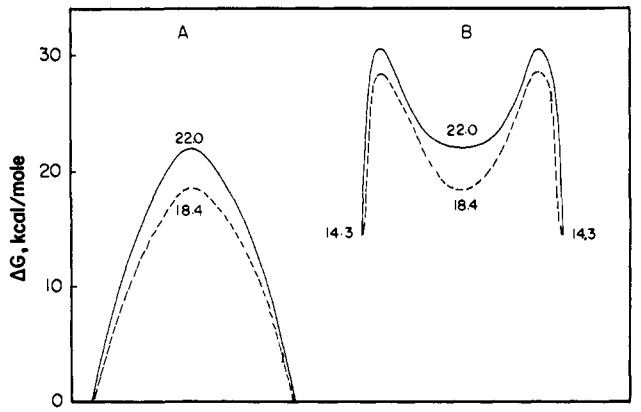

Figure 6. Cross sections through the MOFJ surface for the case shown in Figure 5F (hypothetical X substituent). A, likely cross sections along the reaction coordinate; B, possible cross sections perpendicular to the reaction coordinate. Solid lines, 1,1-dimethoxy complex; dashed lines, spiro complex.

and directions of arrows are arbitrary) which shows arrow 3 or its horizontal component (3′) to be longer for the 1,1-dimethoxy complex. This implies a larger p_{xy} coefficient, as observed.

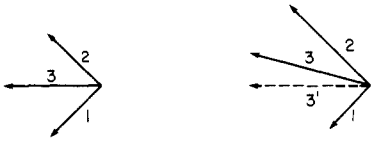

Other reasons for the different p_{xy} values which cannot be excluded at this point include the following.

(1) The difference could be caused by the use of different catalysts (pyridinium ions vs. carboxylic acids). Thus the α values could be affected by the difference in charge[19] and/or a difference in hydrogen-bonding ability of the catalyst. For **4-H**, the only complex whose breakdown is catalyzed by carboxylic acids (α = 0.49) *and* by pyridinium ions (α = 0.38, footnote in Table III), there is indeed a significant difference in the α values. Unless the differences in the charge or in hydrogen-bonding ability change α by the same amount in each reaction this could result in different p_{xy} values in the two families. Change to a medium in which both families of complexes could be studied with a common catalyst type would obviously resolve this ambiguity.

(2) Different curvatures for the two families might arise owing to factors not related to the differences in the barriers, for example, because of different transition-state geometries which could change the structure of the surface. As discussed previously,[1a] one way to explain the lower intrinsic reactivity of the 1,1-dimethoxy complexes is that the transition-state geometry is indeed different from that in the spiro complex reactions in the sense that there is no p–π overlap owing to the wrong orientation of the methoxy groups.

Additional experimental data might possibly help to exclude this possibility as well. As mentioned earlier, the plots of α vs. log K_1 are possibly curved. If this curvature were real this would imply that at some point (for an electron-donating X substituent) there could be an inversion from p_{xy}(spiro) < p_{xy}(1,1-dimethoxy) to p_{xy}(spiro) > p_{xy}(1,1-dimethoxy). Such an inversion in p_{xy} would be difficult to reconcile with the different transition-state geometry being the main cause of the different curvatures. It would, however, be consistent with the above notion of a relationship between barriers and curvatures because the trend toward lower $\Delta\Delta G^{\ddagger}$ with weaker electron-withdrawing substituents (Table VII) suggests that for electron-donating substituents $\Delta\Delta G^{\ddagger}$ will eventually become negative, i.e., show the same sign inversion as p_{xy}. An investigation in a medium such as Me_2SO–water in which Meisenheimer complexes are more stable than in water[2] and in which a wider reactivity range could be studied could probably establish whether p_{xy} is substituent dependent or not.

(3) The above considerations would of course not hold if the lower intrinsic reactivity of the 1,1-dimethoxy complexes was caused by an unfavorable conformational change to a transition state whose geometry is essentially that of the spiro complexes.[1a] In such a case the two energy surfaces would be essentially the same and there would be no obvious reason why p_{xy} should be different for the two families of complexes.

Experimental Section

Materials. All inorganic salts and acetic, formic, methoxyacetic, and chloroacetic acid were analytical grade and used as commercially available. Cyanoacetic acid was recrystallized from chloroform prior to use. Pyridine, 3-chloropyridine, and nicotinamide were purified as described previously.[6] The nitroaromatic compounds were available from a previous study.[1a]

Kinetic Studies. The experimental procedures were the same as described before.[1a]

Acknowledgment. This work was supported by Grants CHE77-27988 and CHE80-24261 from the National Science Foundation. We thank Professor William P. Jencks for criticism and suggestions.

Registry No. 2-H, 85763-25-3; **2-Cl**, 85763-26-4; **2-CF_3**, 85763-27-5; **2-CN**, 85763-28-6; **2-SO_2CH_3**, 85763-29-7; **2-NO_2**, 54524-36-6; **2-SO_2CF_3**, 85763-30-0; **4-H**, 85763-31-1; **4-Cl**, 85763-32-2; **4-CF_3**, 85763-33-3; **4-NO_2**, 85763-34-4; **4-SO_2CF_3**, 85763-35-5; H_2O, 7732-18-5; AcOH, 64-19-7; $MeOCH_2COOH$, 625-45-6; $NCCH_2COOH$, 372-09-8; H_3O^+, 13968-08-6; $NicH^+$, 85763-36-6; PyH^+, 16969-45-2; $PicH^+$, 64711-80-4.